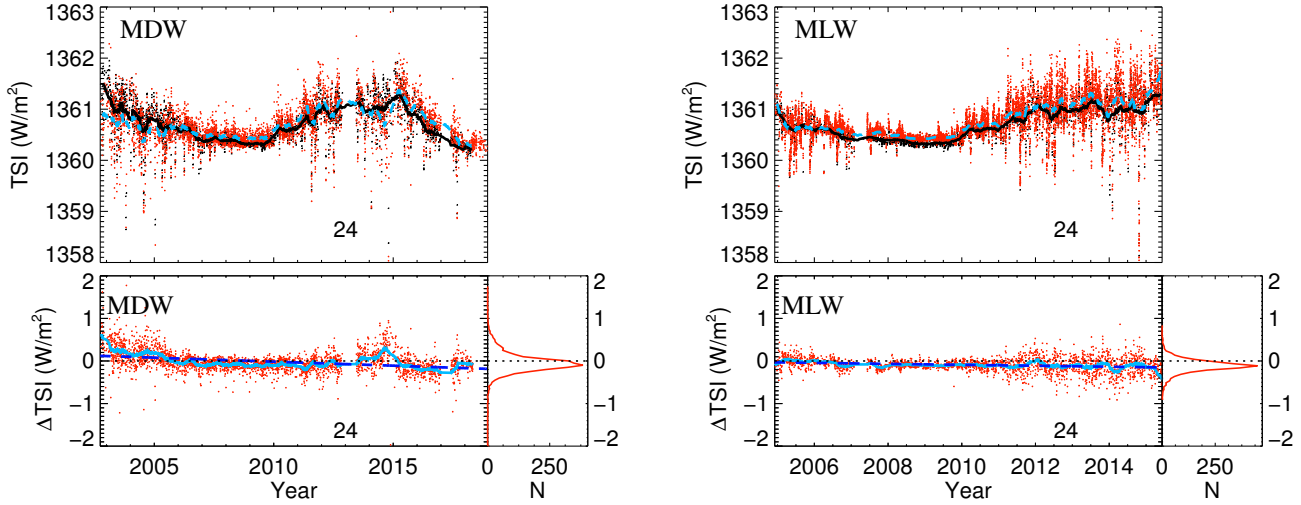

Fig. 7. Same as Fig. 6. but for off-band Ca II K observations from the MDW and MLW datasets (see Sect. 5.2 for more details).

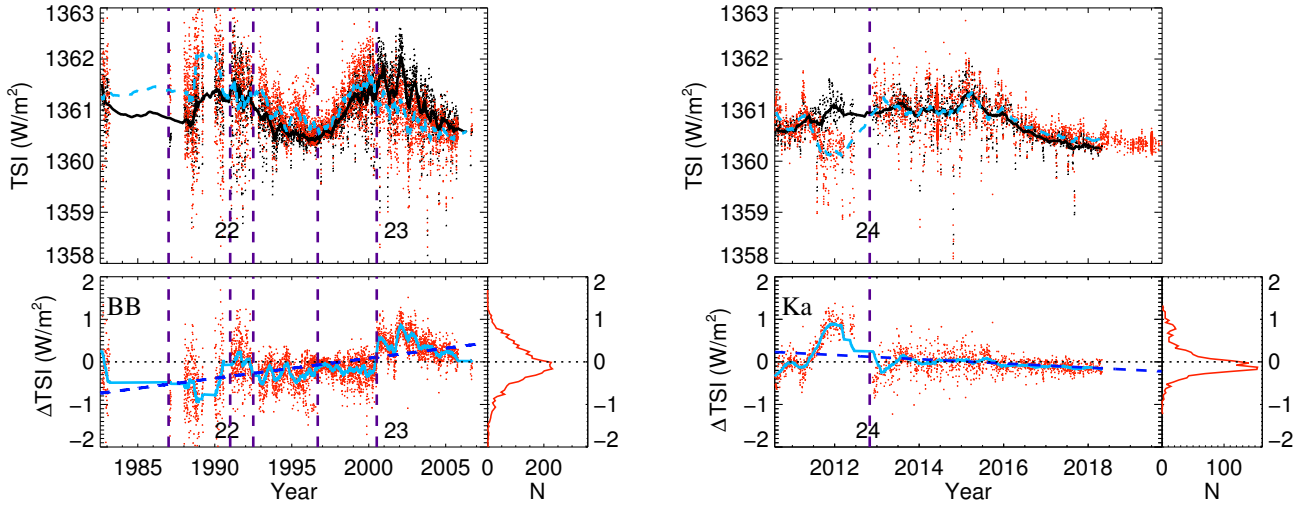

Fig. 8. *Top panels*: daily TSI from the PMOD composite (black) and reconstructed (red) from Ca II K observations from the BB (*left*) and Ka datasets (*right*). Also shown are 81-day running mean values (dashed ciel lines for the reconstructions and black solid lines for the PMOD composite) but only for the days, when both PMOD and the respective reconstruction are available. *Bottom panels*: difference between the PMOD TSI series and the reconstructed TSI. The ciel line shows the 81-day running mean, while the dashed blue line is a linear fit to the residuals. The horizontal dotted black lines denote zero difference. The numbers at the bottom of the panels indicate the solar cycle number and are plotted at roughly the maximum of each cycle. Periods with known instrumental or observational changes are marked with vertical dashed purple lines (see Sect. 5.2 for more details).

reconstructed TSI due to seeing. We stress, however, that this is not a robust measure since it includes contributions from other artefacts plaguing the images too.

5.5. Reconstructions using photographic Ca II K archives

So far, we have considered CCD-based archives. Earlier observations have, however, been stored on photographic plates and films. Compared to CCD observations, analysis of photographic archives involves more intricacies. Their main sources are (1) the non-linear response of photographic material to sunlight exposure, and (2) inconsistencies within the datasets due to changes in the instrumentation and settings for the digitisation unit. Photographic archives have predominantly employed a spectroheliograph, which allows for greater versatility in the observing parameters and many observatories took advantage of this. This, however, resulted in many archives being collections of observations with potentially varying settings. Such changes have not always been noted down or this information has not been transferred to a digital form. Furthermore, inconsistencies within the archives are potentially introduced due to changes and updates in the instrumentation used for the observations. Such inconsistencies are rather common, given the long duration of the observing programmes, which in a few cases, such as MD1, lasted for more than a century. It is worth mentioning that images from photographic archives also suffer from large-scale artefacts. These have, however, been efficiently compensated for by the image processing we had applied to the data

Next, as a fundamental step towards the application of our method to historical Ca II K observations, we now consider two examples of historical photographic archives, MD1 and MW. We focus on the period after 1978, over which direct TSI measurements are available for comparison. The reconstructed TSI from the MD1 and MW archives is shown in Fig. 10, and the results of the quantitative comparison to the PMOD record are listed in Table 6. For comparison, we also reiterate in the

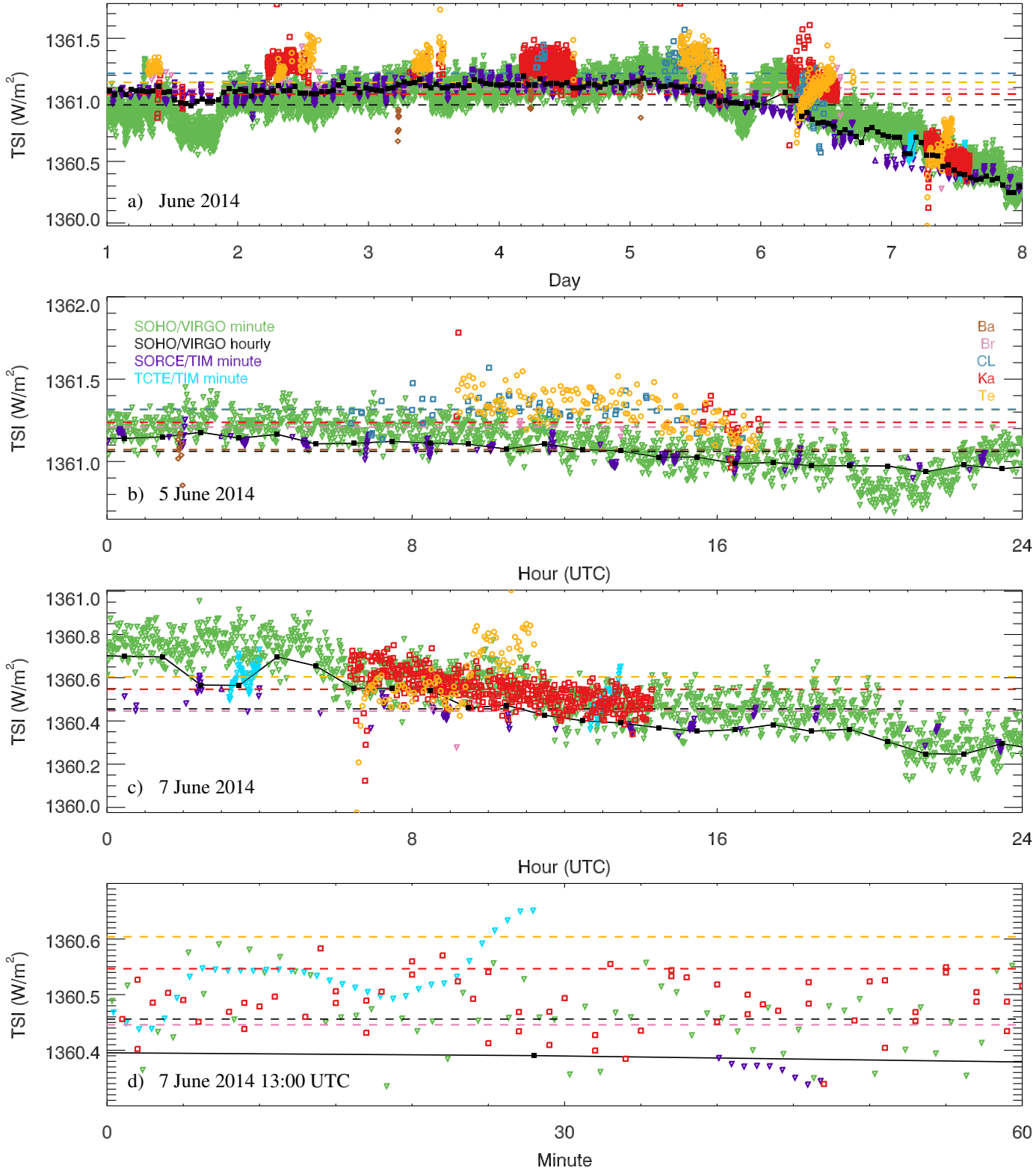

Fig. 9. Reconstructed TSI from Ca II K observations using SOHO/VIRGO data (daily values) as the reference over the course of the first week of June 2014 (*panel a*), on 5 June 2014 (*panel b*), 7 June 2014 (*panel c*), and between 13:00 and 14:00 UTC on 7 June 2014 (*panel d*). The reconstructed TSI is based on the images from Ba (brown rhombuses), Br (pink downward triangles), CL (blue empty squares), Ka (red empty squares), and Te (orange circles). Also shown are the TSI measurements by SOHO/VIRGO (black filled squares connected by the black solid line for hourly values and green downward triangles for data with the cadence of 60 s), SORCE/TIM (purple downward triangles; cadence of 50 s), and TCTE/TIM (ciel downward triangles; cadence of 50 s). In contrast to all other figures where TSI series reconstructed from Ca II K data are shown as daily means over all individual images on that day, here we show the results for each individual image. The horizontal dashed lines mark the mean TSI value of each corresponding series over the specified period, except for panel d, in which the horizontal lines mark the daily mean value.

Table 5. Variability in the measured and reconstructed TSI within one day for the first seven days of June 2014.

	01	02	03	04	05	06	07
SOHO/VIRGO	0.07	0.07	0.07	0.06	0.07	0.07	0.06
SORCE/TIM	0.11	0.06	0.07	0.05	0.06	0.07	0.09
TCTE/TIM	–	–	–	–	–	–	0.11
Ba	–	0.08	0.13	0.09	0.10	–	–
Br	0.04	0.10	–	–	0.03	0.16	0.12
CL	–	–	–	0.09	0.10	0.18	–
Ka	0.14	0.07	0.10	0.07	0.11	0.09	0.07
Te	0.05	0.15	0.12	0.13	0.09	0.18	0.16

Notes. The values are the standard deviations of all reconstructed TSI values within each given day (numbered in the top row) after subtracting a series resulting from 30 min smoothing of the SOHO/VIRGO values in order to take into account the evolution of solar activity.

Table 6. Comparison of TSI reconstructions from the RP and two photographic Ca II K archives to the PMOD TSI composite and SATIRE-S, SATIRE-T, and SATIRE-T2 models.

	PMOD	SATIRE-S	SATIRE-T	SATIRE-T2
RP	0.24 (0.91)	0.24 (0.92)	0.40 (0.76)	0.42 (0.76)
PMOD	–	0.17 (0.98)	0.33 (0.86)	0.38 (0.85)
SF	0.30 (0.84)	0.31 (0.83)	0.42 (0.69)	0.43 (0.70)
PMOD	–	0.18 (0.95)	0.31 (0.83)	0.36 (0.81)
MD1	0.41 (0.77)	0.45 (0.72)	0.56 (0.58)	0.56 (0.61)
PMOD	–	0.24 (0.91)	0.39 (0.77)	0.36 (0.83)
MW	0.43 (0.75)	0.41 (0.74)	0.56 (0.58)	0.54 (0.67)
PMOD	–	0.33 (0.86)	0.47 (0.74)	0.40 (0.83)

Notes. The values are RMS differences in Wm^{-2} followed by R in parentheses. The 2nd line of each section of the table compares SATIRE-S/T/T2 modelled series to PMOD TSI over the same dates as used in the Ca II K archive in question.

table the results for the reconstruction from RP CCD-based observations.

The RMS differences between the reconstructed TSI series and the PMOD record are generally higher for the historical photographic data than for the CCD-based ones. The reconstruction from MW data looks fairly good, with RMS differences to PMOD TSI series of 0.43 Wm^{-2}. Some deviation in the long-term trend is seen, which might be because the considered period (that is over the overlap with satellite TSI data) is quite short to reliably fix the value of the free parameter B_{sat}. Unfortunately, there are also known inconsistencies in the MW series before and after 1976, which makes an extension of this reconstruction further back in time not straightforward. The reconstruction from the MD1 archive is generally of comparable quality to that from MW, although the scatter in the residual is higher during activity maxima. In contrast, the long-term trend is in good agreement with that in PMOD. But the reconstruction exhibits some abrupt changes during known inconsistencies in the data, e.g over 1980 when the digitisation of MD1 data changed, or in 2002 when a CCD camera started being used at MD1.

In Table 6 we also compare our reconstructions from the historical archives and the CCD-based RP archive to that from the SATIRE-S model, which uses the same method but is based on direct magnetograms as well as those from the SATIRE-T and SATIRE-T2 models. To allow for a direct comparison, we also list the RMS difference between the various models and PMOD on the same dates as for the respective Ca II K series. This comparison is restricted to the period prior to 7 November 2008, which is the period covered by all TSI reference series used here. Unsurprisingly, the reconstruction from the observed magnetograms (that is with SATIRE-S) performs better than those from the historic archives. Nevertheless, even with the historic archives, the correlation coefficient with the directly measured TSI is over 0.75. Compared to SATIRE-T/T2 our reconstructions from modern data fare better, while the quality of the reconstructions from historical data is comparable to that of the SATIRE-T/T2 reconstructions.

To summarise, our results show that photographic observations from historical Ca II K archives can be used for past irradiance reconstructions. To allow for reliable reconstructions, however, it is really important to understand and address the various instrumental issues affecting such data, as well as to use observations from multiple archives processed consistently and accurately.

5.6. Sensitivity of reconstruction to reference TSI series

Since most of the historical archives will not have a direct overlap with irradiance measurements, one will have to use intermediate archives to 'cross-calibrate' the reconstructions. Therefore, we also tested whether we can accurately reconstruct TSI when using one of our reconstructed TSI series as the reference. For this, we use the TSI series reconstructed from MD1 Ca II K data, which is the longest series analysed here, as the reference. We note that the MD1 reconstruction was produced by considering Ca II K data stored on photographic plates (before 2002) as well as those taken with a CCD camera (since 2002). We remind that the MD1 reconstruction itself was obtained using PMOD TSI as the reference. The results for six of the archives considered by us are shown in Fig. 11. In the top panel of each block we show the reconstruction for a given archive using MD1 as the reference as well as the PMOD TSI for comparison. The corresponding bottom panels show the difference between the PMOD TSI series and our reconstruction.

Table 3 also lists the obtained B_{sat} value as well as the RMS difference and linear correlation coefficient with the MD1 TSI series. The RMS differences and linear correlation coefficient are given as compared to both the MD1 and the PMOD TSI series. The RMS differences between the series reconstructed with PMOD and MD1 are generally comparable. This is important for employment of the historical Ca II K data for irradiance reconstructions, because it suggests that we can use some of our reconstructed series as a reference for Ca II K archives that do not directly overlap with actual measurements of TSI.

6. Summary and conclusions

Reconstructions of solar irradiance variations on timescales of decades to centuries are usually carried out using sunspot observations. Such observations, however, provide only indirect information on the evolution of the bright magnetic features (faculae or plage, when observed in the photosphere or chromosphere, respectively). Since the late 19th century, the Sun has also been regularly observed in the Ca II K line, whose brightenings directly reflect the presence of plage and network. Consequently, the brightness in this line on the solar disc is a good proxy of the photospheric magnetic field. Due to numerous, partly severe, artefacts and problems affecting such data, the data cannot be used for irradiance or similar studies directly. Chatzistergos et al. (2018b, 2019b) have developed a novel, accurate method to account for most of these problems, which they then applied on images from 43 archives (Chatzistergos et al. 2020c). Next,

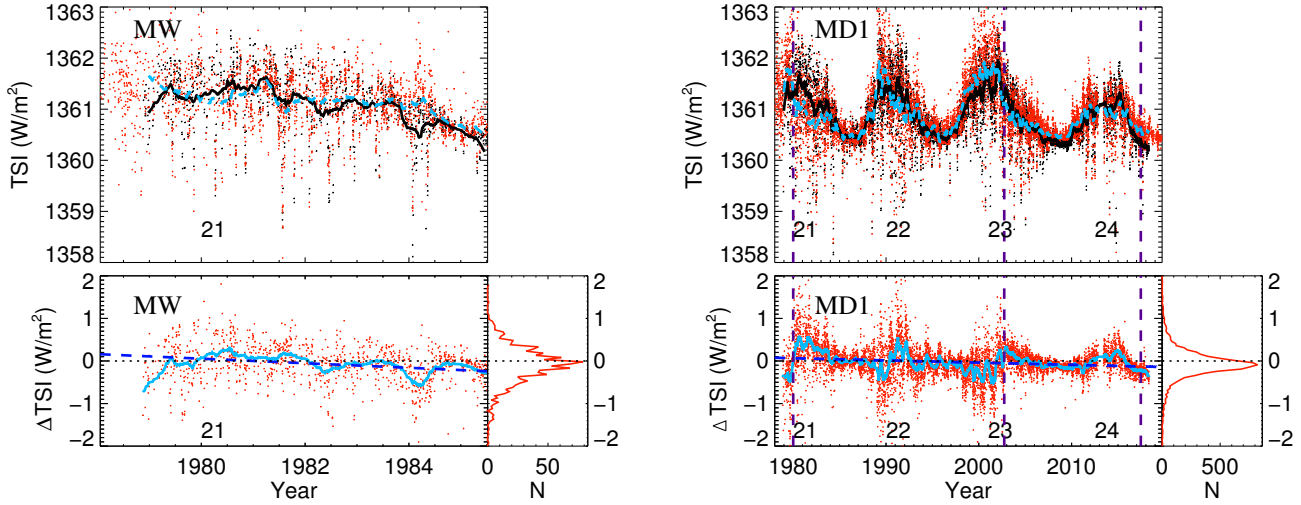

Fig. 10. *Upper part of each panel:* TSI reconstructions from photographic Ca II K observations. Daily values from the MW and MD1 datasets are shown as red dots and the corresponding 81-day running means as dashed blue lines. For comparison, the PMOD irradiance composite series is overplotted (black dots for daily values and the solid black line for the 81-day running means), which was used as the reference for the reconstructed series from MD1 Ca II K data. The running means have been computed considering only days on which both the reconstructions and the PMOD series were available. *Lower left part of each panel:* difference between the PMOD composite and the reconstructed TSI (red dots for daily values and solid light blue for 81-day running means). The dashed blue line is a linear fit to the residuals. The horizontal black dotted line marks the zero difference. *Lower right part of each panel:* distribution of the residuals in bins of 0.05 Wm^{-2}. The numbers in the bottom part of each panel indicate the solar cycle number, which are placed roughly at the maximum of each cycle.

Chatzistergos et al. (2019d) have analysed simultaneous high-quality, high-resolution RP Ca II K and SDO/HMI observations to derive the relationship between the Ca II K brightness and the magnetogram signal.

Here we take the next steps towards exploring the potential of historic solar observations in the Ca II K line for irradiance reconstructions. Using full-disc Ca II K observations from various archives, we reconstructed the TSI back to 1978. To do so, we converted Ca II K observations into unsigned magnetograms by using the relationship by Chatzistergos et al. (2019d) and adapted the SATIRE-S model (Krivova et al. 2003; Yeo et al. 2014), which is normally fed by observed magnetograms, to use the unsigned magnetic maps resulting from the Ca II K images.

We first extensively tested the model by using the modern, high-quality CCD-based Rome/PSPT observations and showed that our model performs at levels comparable to the original SATIRE-S version. We also showed that the reference TSI series, used to fix the free parameter of the model, B_{sat}, does not affect significantly the reconstructed TSI variations. For all independent direct TSI records considered by us as the reference, including TSI composites and measurements by individual instruments, the correlation coefficient with our model and the RMS difference lie in the range 0.90–0.91 and 0.17–0.23 W m^{-2}, respectively (Table 3). The only exception is the ACRIM TSI composite, for which the agreement is significantly poorer, with a correlation coefficient of merely 0.81 and a RMS difference of 0.35 W m^{-2}.

For the period of time covered by Rome/PSPT observations, we can extract sunspot locations and areas from co-temporal red-continuum images. For historical Ca II K archives, this is, unfortunately, not possible. Therefore, we tested different methods for accounting for sunspots by using the record of historical sunspot observations by Mandal et al. (2020). We find only a marginal improvement of the quality of the reconstructions when using co-temporal continuum observations to identify the location and area of sunspots instead of the series by Mandal et al. (2020). This is an important result, because it means we can combine historical sunspot observations with Ca II K image data to reconstruct past irradiance variability with hardly any loss of accuracy.

Next, we employed ten further CCD-based archives to test the effects of the spatial pixel scale, spectral bandpass, changes in properties of the employed instruments, temporal sampling and seeing conditions on the outcome of the model. We estimated the uncertainty in the results due to seeing conditions to generally lie below 0.2 Wm^{-2}. We showed that we can obtain reasonably accurate results even with data with a large pixel scale. This is another advantage of reconstructing solar irradiance with Ca II K observations instead of magnetograms. The amount of detected magnetic flux in magnetograms is strongly diminished with decreasing spatial resolution and the resulting lower net flux due to sub-pixel regions of opposite polarities, while the unsigned magnetograms reconstructed from Ca II K observations are less sensitive to the spatial resolution.

To construct the unsigned magnetograms, we applied to all archives the same relation, which was derived by Chatzistergos et al. (2019d) using RP data. Since some archives employed different bandpasses or used interference filters or spectroheliographs for the observations, this relationship might not be consistent with them. We used Ca II K data with bandwidths covering the entire range of available archives as input, as well as data with bandpasses centred at the wings of the line (off-band), and showed that we could also obtain accurate irradiance reconstructions from such data by adapting the free parameter of the model, B_{sat}. We have, however, noticed a dependence of the adopted value of the free parameter, B_{sat}, on the bandwidth of the Ca II K observations, suggesting that the relationship we use to convert Ca II K data to magnetograms depends on the bandpass. This might potentially be useful for irradiance reconstructions from such archives. A detailed analysis of this effect will be the focus of a forthcoming study.

Further, we present first tests of how well our model works when using historical photographic Ca II K archives. This is an important preparation for the use of the historical Ca II K archives to reconstruct TSI back to the end of the 19th century.